Inelastic tunneling spectroscopy for magnetic atoms and the Kondo resonance

Inelastic tunneling spectroscopy for magnetic atoms and the Kondo resonance

E C Goldberg[1] **and F Flores**[2]

[1] Instituto de Desarrollo Tecnológico para la Industria Química and Departamento de Materiales,
Facultad de Ingeniería Química, CONICET-UNL, Santa Fe, Argentina
[2] Departamento Física Teórica de la Materia Condensada, Universidade Autónoma de Madrid, Madrid,
Spain

E-mail: egold@intec.unl.edu.ar

Abstract

The interaction between a single magnetic atom and the metal environment (including a magnetic field) is analyzed by introducing an ionic Hamiltonian combined with an effective crystal-field term, and by using a Green-function equation of motion method. This approach describes the inelastic electron tunneling spectroscopy and the Kondo resonances as due to atomic spin fluctuations associated with electron co-tunneling processes between the leads and the atom. We analyze in the case of Fe on CuN the possible spin fluctuations between states with $S = 2$ and $3/2$ or $5/2$ and conclude that the experimentally found asymmetries in the conductance with respect to the applied bias, and its marked structures, are well explained by the $2 \leftrightarrow 3/2$ spin fluctuations. The case of Co is also considered and shown to present, in contrast with Fe, a resonance at the Fermi energy corresponding to a Kondo temperature of 6 K.

(Some figures may appear in colour only in the online journal)

1. Introduction

Inelastic tunneling spectroscopy of single magnetic atoms [1–3] and single molecule magnets [4, 5] has recently been used to explore the magnitude, and its anisotropies, of their intrinsic spin. In the single magnetic atom case, Fe, Mn or Co have been deposited on a CuN surface, so that the electrons injected with a STM tip across a single atom interact with the magnetic spin, creating spin-flip processes that reveal themselves in the tip–metal tunneling conductance measured as a function of the bias voltage.

These seminal experiments have been analyzed by different groups, combining an atomic crystal-field effect with an effective interaction between the tunneling electrons and the atomic spin, described by means of an exchange coupling [6, 7], a spin-assisted Hamiltonian [8–11] or using strong coupling theory [12]. All these approaches are reminiscent of the scattering theory approach used by Kondo [13] to explain experimental results concerning the resistivity of dilute magnetic impurities in metals.

Although all these calculations have offered a deep insight into the properties of the scattering mechanism

associated with the interaction of the tunneling electrons and a single magnetic atom, only a few works [7, 15] have addressed the problem of analyzing the low-energy scattering processes related to the corresponding zero bias Kondo resonance; this has been performed starting with an effective spin-assisted Hamiltonian and using either renormalization group techniques [7] (see also [14] for the case of molecular nanomagnets) or third-order perturbation theory in that Hamiltonian [15].

In this paper we reconsider the problem of the inelastic scattering of electrons by a magnetic atom, including the low-energy processes associated with the Kondo resonance (if it exists), by introducing an ionic Hamiltonian [16] to describe the d-electrons of the magnetic atom, and analyze the tunneling current for a metal/atom/tip configuration using a Green-function equation of motion method [17, 18]. In this approach, the inelastic interaction between the incoming electron and the atomic spin is described by means of a co-tunneling process [9], whereby first an electron is injected from one lead into the atom, which changes its electron spin from $S - 1/2$ to S (or from S to $S - 1/2$); in a second step, another electron jumps from the atom into the second lead,

leaving the atom with its initial spin but in a different state (see figure 2 and the corresponding discussion in the text below). As a test of our approach, we discuss first the Fe case, which shows no Kondo effect but presents some interesting asymmetries in the conductance spectra with respect to the applied bias; in a second example we consider Co and analyze its Kondo resonance.

2. Theory

Our starting point is the following ionic Hamiltonian including all the atom d-orbitals:

$$
\begin{aligned}
H = &\sum_{k,\alpha,\sigma} \varepsilon_{k\alpha} \hat{c}^{+}_{k\alpha\sigma} \hat{c}_{k\alpha\sigma} + H_{\text{atom}} \\
&+ \sum_{k,\alpha,m,\sigma} (V_{k\alpha m} \hat{c}^{+}_{k\alpha\sigma} \hat{c}_{m\sigma} + \text{c.c.}).
\end{aligned} \tag{1}
$$

The first term in equation (1) describes the electrons of the leads, $\hat{c}^{+}_{k\alpha\sigma}$ ($\hat{c}_{k\alpha\sigma}$) being the creation (annihilation) operator associated with the state $k\alpha\sigma$ ($\alpha = 1, 2$ refers to the tip and the metal, respectively); H_{atom} describes the d-electrons of the atom and the last term the interaction between the leads and the atom (H_{int}). In this term, $V_{k\alpha m}$ defines the coupling between the conduction, $k\alpha\sigma$, and the localized, $m\sigma$, electrons; $\hat{c}^{+}_{m\sigma}$ ($\hat{c}_{m\sigma}$) denotes the creation (annihilation) operator of the localized d-electrons in the orbital m with spin σ.

The critical point is the description of the d-electrons, and this point marks an important difference of our proposal with respect to other works based on an effective exchange coupling of the atomic spin to the reservoirs [6–11]. For the free atom we consider the following Hamiltonian:

$$
\begin{aligned}
H^{0}_{\text{atom}} = &\sum_{m,\sigma} \varepsilon_{m} \hat{n}_{m\sigma} + \sum_{m} U_{d} \hat{n}_{m\uparrow} \hat{n}_{m\downarrow} \\
&+ \frac{1}{2} \sum_{m\neq m',\sigma} J_{d} \hat{n}_{m\sigma} \hat{n}_{m'-\sigma} \\
&+ \frac{1}{2} \sum_{m\neq m',\sigma} (J_{d} - J^{x}_{d}) \hat{n}_{m\sigma} \hat{n}_{m'\sigma} \\
&- \frac{1}{2} \sum_{m\neq m',\sigma} J^{x}_{d} \hat{c}^{+}_{m\sigma} \hat{c}_{m-\sigma} \hat{c}^{+}_{m'-\sigma} \hat{c}_{m'\sigma}.
\end{aligned}
$$

Here, in the expression of H^{0}_{atom}, $\hat{n}_{m\sigma} = \hat{c}^{+}_{m\sigma} \hat{c}_{m\sigma}$ and the intra-atomic Coulomb interactions U_{d} and J_{d}, as well as the intra-atomic exchange interaction J^{x}_{d}, are assumed to be constants independent of the m-orbital index. The last term, related to spin-flip processes, restores the invariance under rotation in spin space.

A crucial approximation to analyze H^{0}_{atom} and its interaction with the leads is to assume the exchange interaction, J^{x}_{d}, to be large enough to make the first Hund-rule operative. Then, the atomic lower energy configurations correspond to the states of maximum electron spin, say S. Consider the Fe case; DFT calculations [7] for this atom on CuN(100) show that the electron charge in the d-states is between 6 and 7, suggesting that the atomic spin fluctuates between 2 (six electrons) and 3/2 (seven electrons). Those DFT calculations also indicate that the largest occupancies appear for the d_{x2-y2} and d_{z2} orbitals, with occupancies for
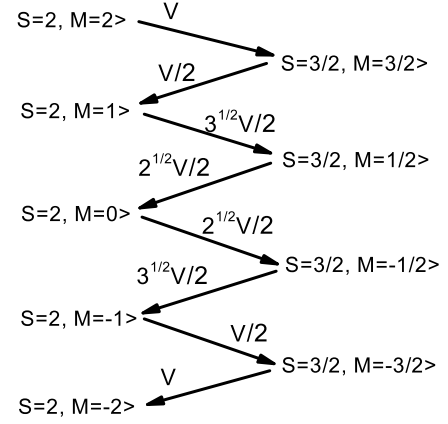

Figure 1. Diagram of the processes that change the atom spin between $S = 2$ and $S = 3/2$, with the hopping elements normalized to the maximum value.

the minority spin of 0.72 and 0.49 electrons, respectively. We describe the atomic states of Fe with $S = 2$ or $3/2$ by means of different kets associated with the d-orbitals, $|d_{x2-y2}, d_{z2}, d_{zy}, d_{xy}, d_{zx}\rangle$, in the following way (including also spin variables):

$$
\begin{aligned}
|S = 2, M = 2\rangle = &| \uparrow\downarrow, \uparrow 0, \uparrow 0, \uparrow 0, \uparrow 0\rangle \\
|S = 2, M = 1\rangle = &\tfrac{1}{2}[| \uparrow\downarrow, 0\downarrow, \uparrow 0, \uparrow 0, \uparrow 0\rangle \\
&+ | \uparrow\downarrow, \uparrow 0, 0\downarrow, \uparrow 0, \uparrow 0\rangle + | \uparrow\downarrow, \uparrow 0, \uparrow 0, 0\downarrow, \uparrow 0\rangle \\
&+ | \uparrow\downarrow, \uparrow 0, \uparrow 0, \uparrow 0, 0\downarrow,\rangle]\dots \\
|S = 2, M = -2\rangle = &| \uparrow\downarrow, 0\downarrow, 0\downarrow, 0\downarrow, 0\downarrow\rangle
\end{aligned} \tag{2a}
$$

and:

$$
\begin{aligned}
|S = 3/2, M = 3/2\rangle = &| \uparrow\downarrow, \uparrow\downarrow, \uparrow 0, \uparrow 0, \uparrow 0\rangle \\
|S = 3/2, M = 1/2\rangle = &\frac{1}{\sqrt{3}}[| \uparrow\downarrow, \uparrow\downarrow, 0\downarrow, \uparrow 0, \uparrow 0\rangle \\
&+ | \uparrow\downarrow, \uparrow\downarrow, \uparrow 0, 0\downarrow, \uparrow 0\rangle + | \uparrow\downarrow, \uparrow\downarrow, \uparrow 0, \uparrow 0, 0\downarrow\rangle] \\
\dots & \\
|S = 3/2, M = -3/2\rangle = &| \uparrow\downarrow, \uparrow\downarrow, 0\downarrow, 0\downarrow, 0\downarrow\rangle.
\end{aligned} \tag{2b}
$$

The effect of the atom–leads interactions is to make electrons jump between the leads and the atom, changing the atom state between $S = 2$ and $3/2$. All these processes are indicated schematically in figure 1. Notice that by injecting (or removing) one electron in (from) the atom, the value of M can only change by $\pm 1/2$, depending on the spin of the electron. Moreover, using the atom–leads interaction (H_{int}) we can calculate the matrix elements associated with the different processes shown in this figure. This allows us to write H^{0}_{atom} and H_{int} as follows [17]:

$$
\begin{aligned}
H^{0}_{\text{atom}} = &\sum_{M} \varepsilon_{S} |S, M\rangle \langle S, M| \\
&+ \sum_{m} \varepsilon_{S-1/2} |S - 1/2, m\rangle \langle S - 1/2, m| \\
H_{\text{int}} = &\sum_{k,\alpha,M,\sigma} \left[V_{k\alpha M\sigma} \hat{c}^{+}_{k\alpha\sigma} |S, M\rangle \langle S - 1/2, M - \sigma| + \text{c.c.} \right].
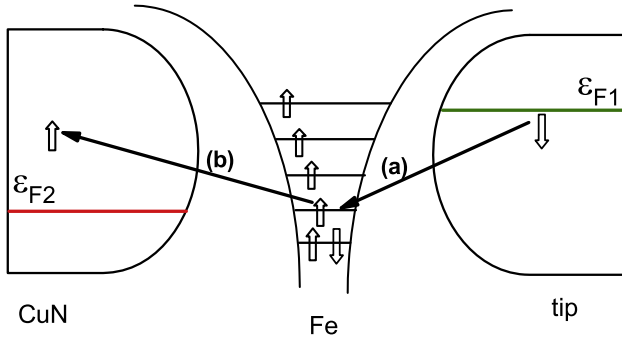\end{aligned} \tag{2c}
$$

Figure 2. In this figure we show a co-tunneling process for Fe: (a) with one electron jumping from the tip to the d_{z^2}-orbital (spin down) and, (b) with the electron of spin up jumping from the same orbital to CuN. In this process the atomic spin changes from $S = 2$, $M = 2$ to $S = 2$, $M = 1$, and it fluctuates to $S = 3/2$, $M = 3/2$.

Here we find that [17] $V_{k\alpha M\sigma} = \sqrt{\frac{5(S+M*\text{sign}(\sigma))}{2S}} V_{k\alpha}$, $\sqrt{5}V_{k\alpha}$ being the interaction between the $k\alpha$-wavefunction and the d_{z^2}-state that yields the atomic $2 \leftrightarrow 3/2$ transitions as defined by the wavefunctions (2a) and (2b).

It is interesting to note that a similar interacting Hamiltonian, as given by equation (2c), is obtained if instead of $|S = 2, M = 2\rangle = |\uparrow\downarrow, \uparrow 0, \uparrow 0, \uparrow 0, \uparrow 0\rangle$, we assume we have:

$$|S = 2, M = 2\rangle = \alpha|\uparrow\downarrow, \uparrow 0, \uparrow 0, \uparrow 0, \uparrow 0\rangle$$
$$+ \beta|\uparrow 0, \uparrow\downarrow, \uparrow 0, \uparrow 0, \uparrow 0\rangle$$

for the atomic ground state, with the $d_{x^2-y^2}$ state occupancy fluctuating with the atomic spin fluctuations $2 \leftrightarrow 3/2$, as well. The only change we find in this case for the interacting Hamiltonian appears in $V_{k\alpha}$, which is now an average of the hopping interactions between $k\alpha$ and the d_{z^2} and $d_{x^2-y^2}$ states.

The arguments presented above for the Fe case can be generalized to other magnetic atoms; in this way we find that equation (2c) holds for all these cases if the d-shell occupancy is more than half filled. In the other limit, for an atomic d-shell having less than half-filled occupancy, H_{int} in equation (2c) should be changed to:

$$H_{\text{int}} = \sum_{\substack{k,\alpha,\\M,\sigma}} \left[V_{k\alpha M\sigma} \hat{c}^+_{k\alpha\sigma} |S - 1/2, M - \sigma\rangle\langle S, M| + \text{c.c.} \right]; \quad (3)$$

this shows that there is an electron–hole symmetry between the cases having either more or less than a half-filled shell. In the following we shall work with holes for Fe or Co, using H_{int} as given by equation (3).

We should also mention that in this way of proceeding, the current across the magnetic atom is the result of a co-tunneling process whereby two electrons are tunneling between the leads and the magnetic atom: in a first step, an electron tunnels from the atom to one of the leads and, in a second step, another electron jumps from the second lead to the atom (see figure 2).

All eigenstates $|S, M\rangle$ of Hamiltonians (2c) and (3) are degenerate in M. This degeneracy is broken by the crystal-field effect that is obtained by adding to H^0_{atom} the Zeeman plus the anisotropy energy [1]:

$$H_{\text{atom}} = H^0_{\text{atom}} + g\mu_B \hat{B} \cdot \hat{S} + D\hat{S}_z^2 + E(\hat{S}_x^2 - \hat{S}_y^2). \quad (4)$$

In equation (4) E and D are two constants describing the crystal-field effect; the gyromagnetic factor is g and μ_B is the Bohr magneton. $\hat{S}$ is the spin operator of the adsorbate and $\hat{S}_{x,y,z}$ its projections on Cartesian axes.

In the basis set diagonalizing H_{atom}, $\varphi_i^S = \sum_M a^i_{S,M}|S, M\rangle$ and $\varphi_j^{S-1/2} = \sum_M a^j_{S-1/2,M}|S - 1/2, M\rangle$ with eigenvalues E_i^S and $E_j^{S-1/2}$, H_{int} can be written as follows:

$$H_{\text{int}} = \sum_{k,\alpha,M,\sigma} \left[V_{k\alpha M\sigma} \hat{c}^+_{k\alpha\sigma} \sum_j |\varphi_j^{S-1/2}\rangle\langle\varphi_j^{S-1/2}| \right.$$
$$\times |S - 1/2, M - \sigma\rangle$$
$$\left. \times \sum_i \langle S, M||\varphi_i^S\rangle\langle\varphi_i^S| + \text{c.c.} \right]$$
$$= \sum_{k,\alpha,\sigma,i,j} \left[T_{k\alpha\sigma ji} c^+_{k\alpha\sigma} |\varphi_j^{S-1/2}\rangle\langle\varphi_i^S| + \text{c.c.} \right]. \quad (5)$$

The coupling term introduced in equation (5) is defined as

$T_{k\alpha\sigma ji}$
$$= \sum_M a^{j*}_{S-1/2,M-\sigma} a^i_{S,M} \sqrt{(5/2S)(S + M * \text{sign}(\sigma))} V_{k\alpha}. \quad (6)$$

Due to the anisotropy effects, this coupling acts between all the different φ_i^S and $\varphi_j^{S-1/2}$ states into which the degenerate levels, $|S \cdot M\rangle$ or $|S - 1/2, m\rangle$ are split.

A Keldysh–Green function approach [19] is a convenient way of treating out-of-equilibrium problems such as the one posed by the inelastic tunneling current effects through the magnetic atom. In our analysis, we use Hamiltonian equation (1) written in the basis set φ_i^S and $\varphi_j^{S-1/2}$ and introduce the following Green functions:

$G_{ij}(t, t')$
$$= i\Theta(t' - t)\left\langle\left\{|\varphi_i^S\rangle\langle\varphi_j^{S-1/2}|_{t'}; |\varphi_j^{S-1/2}\rangle\langle\varphi_i^S|_t\right\}\right\rangle;$$
$$F_{ij}(t, t') = i\left\langle\left[|\varphi_i^S\rangle\langle\varphi_j^{S-1/2}|_{t'}; |\varphi_j^{S-1/2}\rangle\langle\varphi_i^S|_t\right]\right\rangle,$$

where {}/[] indicates the anticommutator/commutator of the corresponding operators defined in t' and t; the function F is the specific Green function yielding the non-equilibrium properties of the system. G and F have been calculated using the equation of motion method up to second order in the interaction $T_{k\alpha\sigma ji}$. By following the steps already discussed in [17, 18], one arrives at the following Green function:

$$G_{ij}(\omega) = \begin{cases} \langle n_i^S + n_j^{S-1/2}\rangle \\ \\ + \sum_{\substack{k,\alpha,\sigma \\ m \neq j}} \frac{T_{k\alpha\sigma mi}\langle|\varphi_i^S\rangle\langle\varphi_m^{S-1/2}|c_{k\sigma}\rangle}{\tilde{\omega} - \varepsilon_{k\alpha} - E_m^{S-1/2} + E_j^{S-1/2}} \end{cases}$$

$$- \sum_{\substack{k,\alpha,\sigma \\ m \neq i}} \frac{T_{k\alpha\sigma jm} \langle |\varphi_m^S \rangle \langle \varphi_j^{S-1/2}|c_{k\sigma}\rangle}{\tilde{\omega} - \varepsilon_{k\alpha} - E_i^S + E_m^S} \Bigg\}$$

$$\times \Bigg\{ \tilde{\omega} - E_i^S + E_j^{S-1/2} - \sum_{k,\alpha,\sigma} \frac{|T_{k\alpha\sigma ji}|^2}{\tilde{\omega} - \varepsilon_{k\alpha}}$$

$$- \sum_{\substack{k,\alpha,\sigma \\ m \neq i}} \frac{|T_{k\alpha\sigma jm}|^2 \langle n_{k\alpha\sigma}\rangle}{\tilde{\omega} - \varepsilon_{k\alpha} - E_i^S + E_m^S}$$

$$- \sum_{\substack{k,\alpha,\sigma \\ m \neq j}} \frac{|T_{k\alpha\sigma mi}|^2 \langle 1 - n_{k\alpha\sigma}\rangle}{\tilde{\omega} - \varepsilon_{k\alpha} - E_m^{S-1/2} + E_j^{S-1/2}} \Bigg\}^{-1} \quad (7)$$

where $\langle n_{k\alpha\sigma}\rangle (= f_{\alpha<}(\omega))$ is the Fermi distribution function for the $k\alpha$-states and $\varpi = \omega - i\eta$ with $\eta \to 0$. All the calculations described below are done for $T = 0.5$ K; due to this low temperature and the weak surface–atom coupling (see below) we find a negligible occupation of the atomic excited levels, $\langle n_i^S \rangle$ or $\langle n_j^{S-1/2} \rangle$. Close to the equilibrium and within a second order in the interaction $T_{k\alpha\sigma ji}$, the crossed terms (namely $\langle |\varphi_i^S \rangle \langle \varphi_m^{S-1/2}|c_{k\sigma}\rangle$ and $\langle |\varphi_m^S \rangle \langle \varphi_j^{S-1/2}|c_{k\sigma}\rangle$) appearing in the numerator of equation (7) are given by:

$$\langle |\varphi_i^S \rangle \langle \varphi_n^{S-1/2}|c_{k\alpha\sigma}\rangle$$
$$\simeq \frac{1}{\pi} T_{k\alpha\sigma ni}^* \int_{-\infty}^{\infty} d\omega' f_{\alpha<}(\omega') \mathrm{Im} \frac{G_{in}(\omega')}{\tilde{\omega}' - \varepsilon_{k\alpha}}.$$

We should stress that equation (7) yields the advanced Green function for a less than half-filled shell; the case for more than five d-electrons in the atom can be described using the electron–hole symmetry of the problem, by reversing in equation (7) the sign of all the energies.

The tip-metal current I_α^σ, calculated across the α-contact, is defined by the equation:

$$I_\alpha^\sigma = -\frac{2e}{\hbar} \mathrm{Im} \sum_{k,i,j} T_{k\alpha\sigma ji}^* \langle |\varphi_i^S \rangle \langle \varphi_j^{S-1/2}|c_{k\alpha\sigma}\rangle, \quad (8)$$

which can be written in terms of G_{ij} and F_{ij} as follows [18]:

$$\frac{I_\alpha^\sigma}{2e/h} = \frac{1}{2} \sum_{i,j} \int_{-\infty}^{\infty} d\varepsilon \, \Gamma_{\alpha\sigma ji}(\varepsilon) \mathrm{Im}[F_{ij}(\varepsilon)$$
$$- 2(2f_{\alpha<}(\varepsilon) - 1)G_{ij}(\varepsilon)] \quad (9)$$

where we have introduced $\Gamma_{\alpha\sigma ji}(\varepsilon) = \pi \sum_k |T_{k\alpha\sigma ji}|^2 \delta(\varepsilon - \varepsilon_{k\alpha})$. In equation (8), $I_\alpha^\sigma = \sum_{i,j} I_{\alpha ij}^\sigma$, $I_{\alpha ij}^\sigma$ represents a partial current associated with the (i,j)-channel. Current conservation for each channel, $I_{1ij}^\sigma = -I_{2ij}^\sigma$, allows us to write equation (9) as follows:

$$\frac{I_\sigma}{2e/h}$$
$$= \sum_{i,j} \int_{-\infty}^{\infty} d\varepsilon \, \Gamma_{\sigma ji} [f_{1<}(\varepsilon) - f_{2<}(\varepsilon - eV)] \, \mathrm{Im}G_{ij}(\varepsilon), \quad (10)$$

where $\Gamma_{\sigma ji} = 2\Gamma_{1\sigma ji}\Gamma_{2\sigma ji}/(\Gamma_{1\sigma ji} + \Gamma_{2\sigma ji})$ defines an effective broadening associated with the $T_{k\alpha\sigma ji}$-hoppings.

Equation (10) is similar to the one proposed by Meir and Wingreen [20]; but in our approach we find a combination of similar contributions for the different (i,j)-channels. Equations (7) and (10) summarize the properties of the magnetic atoms as described in this paper: while equation (7) yields the characteristics of the spectral density, equation (10) yields its transport properties. The conductance ($G = \mathrm{d}I/\mathrm{d}V$), in the limit of low temperatures and small bias voltages, can be approximated by the expression $G/G_0 = \sum_{i,j,\sigma} \Gamma_{\sigma ji} \mathrm{Im}G_{ij}(eV)$, G_0 being the conductance quantum.

It is interesting to consider the limit of no crystal-field effect ($E = D = 0$) and zero magnetic field ($B = 0$). In this case the following two terms that include the factor $\langle n_{k\alpha\sigma}\rangle$ in equation (7),

$$\sum_{\substack{k,\alpha,\sigma \\ m \neq i}} \frac{|T_{k\alpha\sigma jm}|^2 \langle n_{k\alpha\sigma}\rangle}{\tilde{\omega} - \varepsilon_{k\alpha} - E_i^S + E_m^S}$$
$$- \sum_{\substack{k,\alpha,\sigma \\ m \neq j}} \frac{|T_{k\alpha\sigma mi}|^2 \langle n_{k\alpha\sigma}\rangle}{\tilde{\omega} - \varepsilon_{k\alpha} - E_m^{S-1/2} + E_j^{S-1/2}}, \quad (11)$$

reduce to $(5/2S) \sum_{k\alpha} |V_{k\alpha}|^2 \langle n_{k\alpha\sigma}\rangle/(\tilde{\omega} - \varepsilon_{k\alpha})$, which can be associated with a Kondo resonance if $\varepsilon_S - \varepsilon_{S-1/2} < 0$ (electron picture) [16]. The effect of the environment on the magnetic atom is to split ε_S and $\varepsilon_{S-1/2}$ into the levels E_i^S and $E_j^{S-1/2}$, and the Kondo resonance into the different structures afforded by the two terms of equation (11). Notice that the different energies, $E_i^S - E_m^S$ and $E_m^{S-1/2} - E_j^{S-1/2}$, are associated with the excitation energies of the magnetic atom, either for the spin S ($i \to m$) or the spin $S - 1/2$ ($m \to j$), as created by the co-tunneling processes included in our Hamiltonian. Moreover, for $\varepsilon_S - \varepsilon_{S-1/2} < 0$ and $E_i^S = E_m^S$, the first term of equation (11) yields a Kondo resonance, while for $E_j^{S-1/2} = E_m^{S-1/2}$, the second term yields in our calculations a small depression in the density of states, referred to, in this paper, as an anti-resonance.

3. Results and discussion

We first discuss the case of Fe on CuN [1]; the ground state has six d-electrons (four holes) with $S = 2$, and following [1] we take in Hamiltonian (5) $g = 2.11$, $D = -1.55$ meV and $E = 0.31$ meV. For the sake of completeness we have explored the different possible spin fluctuations for Fe by considering two cases: $2 \leftrightarrow 3/2$ or $2 \leftrightarrow 5/2$, with the atom fluctuating between two spins by taking (donating) one electron from (to) the substrate. In the ionic Hamiltonian for the hole fluctuations, these cases correspond to taking: $\varepsilon_{S=2} - \varepsilon_{S=3/2} > 0$ or $\varepsilon_{S=5/2} - \varepsilon_{S=2} < 0$. The α-lead–atom interaction width is defined by the quantity $\Gamma_\alpha = \pi \sum_k |V_{k\alpha}|^2 \delta(\varepsilon - \varepsilon_{k\alpha})$. The atom–tip interaction Γ_1 is negligible compared with the atom–metal one Γ_2, therefore it is a good approximation to take $\Gamma_{\sigma ji} = 2\eta_{\sigma ji}\Gamma_1$ with $\eta_{\sigma ji} = |\sum_M a_{S-1/2,M-\sigma}^{j*} a_{S,M}^i \sqrt{(5/2S)(S + M * \mathrm{sign}(\sigma))}|^2$. Then the conductance results from the different contributions, which are determined basically by the atom–surface interaction,
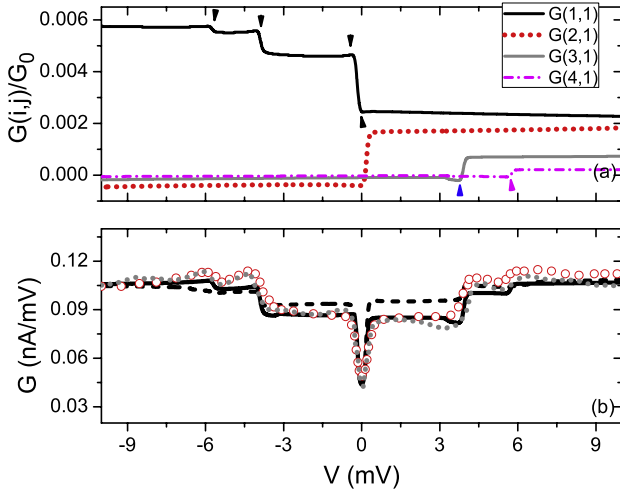
Figure 3. (a) shows the most important contributions, $G(i, j)$, to the differential conductance in G_0-units for Fe and the $2 \leftrightarrow 3/2$ fluctuating case (see text) (in Fe, $G(i, 1) = G(i, 2)$ and $G(5, 1)$ is negligible). The arrows show the energies associated with the energy steps. (b) shows the differential conductance for the $2 \leftrightarrow 3/2$ (black curve) and the $2 \leftrightarrow 5/2$ (dashed line) spin fluctuations. Red circles [1] and gray dot line (supporting online material of [1]) show the experimental data for a zero magnetic field.

but weighted by the strength of the atom–tip coupling. In our calculations we use a flat band approximation with a half-bandwidth of $\Lambda = 10$ eV, and the values $\varepsilon_{S=2} - \varepsilon_{S=3/2} = \varepsilon_{S=2} - \varepsilon_{S=5/2} = 2$ eV, $\Gamma_2 = 32$ meV and $\Gamma_1 = 2.2$ meV, which were chosen in order to adjust the experimental conductance curve in the absence of a magnetic field ($B = 0$ T) (for $D = E = 0$, these values yield a d-level broadening of 0.2 eV).

In part (a) of figure 3, we show for the $2 \leftrightarrow 3/2$ spin fluctuating case the most important contributions to the conductance associated with the terms $2\eta_{\sigma ji}\text{Im}G_{ij}$ (eV). In all these cases the step structures correspond to the excitations between the hole ground state, 6.4 meV, and the other excited levels (conductance steps are associated with the excitation energies 0.2, 3.9, 5.7 and 6.6 meV for $S = 2$). The most important contributions to the conductance are provided by the Green functions G_{11} ($=G_{12}$) and G_{m1} ($=G_{m2}$), with $m = 2, 3, 4$, shown in the panel (a) of figure 3 ($i = 1$ defines the ground state for $S = 2$ and $j = 1, 2$ the ground degenerate levels for $S = 3/2$; for this case, $E_j^{3/2} = 3.6, 3.6, 0.3$ and 0.3 meV).

It is interesting to realize that G_{11} (or G_{12}) yields that important contribution because of the ground state occupancy $\langle n_1^S \rangle \sim 1$ (see equation (7)); this leads to all the steps for $\omega = E_1^S - E_m^S$ associated with $\sum_{k,\alpha,\sigma \atop m \neq i} \frac{|T_{k\alpha\sigma j m}|^2 \langle n_{k\alpha\sigma} \rangle}{\tilde{\omega} - \varepsilon_{k\alpha} - E_1^S + E_m^S}$ because, for that occupancy, in the Green functions G_{11} or G_{12} the magnetic atom is excited from the $\varphi_1^{S=2}$ state to an intermediate state $\varphi_m^{S=3/2}$ (as created by the transfer of one electron from one contact to the atom); in the second co-tunneling step, the atom jumps to a $\varphi_{m \neq 1}^{S=2}$ state (with one electron being transferred from the atom to the other contact).

On the other hand, for G_{m1}, with $m \neq 1$, we find $\langle n_m^S \rangle \sim 0$ in equation (7); however, for this case the crossed term

$\langle |\varphi_1^S\rangle \langle \varphi_1^{S-1/2}|c_{k\alpha\sigma}\rangle$ provides the relevant contribution that makes G_{m1} important. In this case, in the Green function G_{m1} the magnetic atom is excited from the $\varphi_{m\neq 1}^{S}$ state to $\varphi_m^{S=3/2}$ (when an electron is injected in the atom), while in a second step the atom jumps to the $\varphi_1^{S=2}$ state (and one electron is transferred to the other lead). This leads to the step frequencies $\omega = E_m^S - E_1^S$, just the opposite of the ones found for G_{11} or G_{12}. The steps associated with G_{11} or G_{m1} are not, however, exactly symmetric with respect to each other because of the different weights associated with the corresponding Green functions, depending on either $\langle n_1^S\rangle$ for G_{11} or $(-\sum_{k,\alpha,\sigma} \frac{T_{k\alpha\sigma 11}\langle|\varphi_1^S\rangle\langle\varphi_1^{S-1/2}|c_{k\sigma}\rangle}{\tilde{\omega}-\varepsilon_{k\alpha}-E_m^S+E_1^S})$ for G_{m1}. Then, our model predicts an asymmetric behavior in the bias voltage of the conductance (see figure 1), in agreement with the experimental findings [1]. On the other hand, we find that the small structures appearing at ± 3.3 meV are associated with virtual excitations between the spin $S = 3/2$ states. It is interesting to realize that, in the presence of a crystal field, a Kondo resonance or an anti-resonance emerge when the crystal field creates degenerate S and/or $S - 1/2$ ground states. In the case of Fe on CuN there is no degenerate ground state for $S = 2$ and, consequently, there is no Kondo resonance, while a small anti-resonance structure associated with the second term of equation (11) appears due to the degeneration for the $S = 3/2$ states, as can be seen from figure 3. The resulting conductance spectrum is presented in panel (b), where we compare the two possible spin fluctuations, $2 \leftrightarrow 3/2$ and $2 \leftrightarrow 5/2$, with the experimental evidence [1] (including the one presented in the supporting online material [1]). Notice the more pronounced structures and the asymmetric behavior afforded by the $2 \leftrightarrow 3/2$ case, in better agreement with those data.

The strong dependence of the spin excitations on field direction observed experimentally is also well reproduced by our calculations, as can be seen from figure 4. Figure 4 shows the conductance as a function of the bias voltage for different values of the applied magnetic field B along the N direction (B_z) in part (a) and along the hollow direction (B_x) in part (b). The behavior is the same as observed experimentally, three ($1 \rightarrow 2$, $1 \rightarrow 3$ and $1 \rightarrow 4$) of the four steps associated with the excitations from the lower energy eigenstate of the crystal field Hamiltonian for $S = 2$ appear at the predicted threshold energies (see figures 4(a) and (b)). In the case of B along the N direction, the $1 \rightarrow 2$ excitation dominates at very low B and disappears when B increases, whereas $1 \rightarrow 3$ dominates at large B. The step energies extracted from the conductance spectra of figure 4 are also in very good agreement with the experimental values. We should also mention that in this paper we have only considered magnetic fields up to 7 T, as measured in the experimental data; this leaves apart a possible Kondo effect that has been suggested [7] to appear for higher fields along the x-axis, due to the crossing of two atomic levels for $S = 2$.

The case of Co ($S = 3/2$) [2] is particularly interesting because of the twofold degeneracy associated with the $M = \pm 1/2$ ground states, which appear due to the hard-axis anisotropy ($D > 0$). This suggests that a Kondo resonance
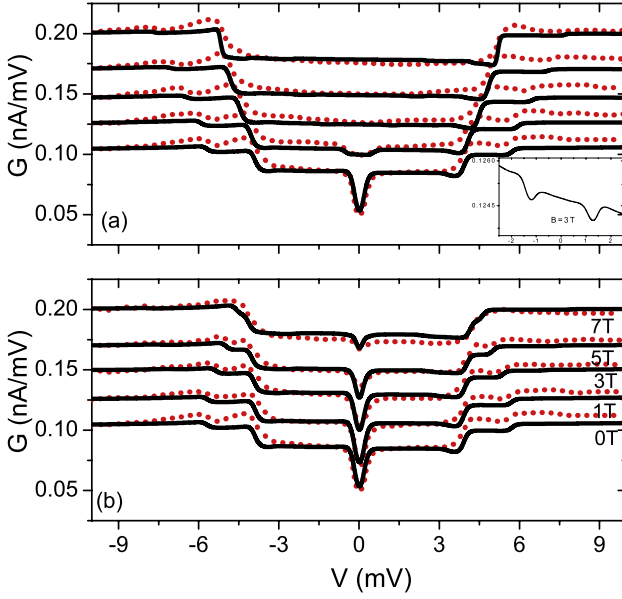
Figure 4. Computed conductance for a Fe atom on a CuN monolayer on Cu(100). The conductance for increasing magnetic field B is vertically displaced for representation purposes. The B field is oriented along the N axis in part (a) and along the hollow axis on the surface in part (b). The dotted curves are the experimental results of [1]. The inset in (a) shows an expanded view of the theoretical curve around $V = 0$ mV in the case of $B = 3$ T to show that the 1–2 excitation still exists at an energy of 1.5 meV, in agreement with the experiment.

Figure 5. Computed conductance (full line) for a Co atom on a CuN monolayer on Cu(100). The conductance for increasing magnetic fields along the hollow axis (z) is vertically displaced for representation purposes. Our theoretical Kondo resonance is smaller than the experimental one [2] (dotted line) because of our second-order approximation in the equation of motion method. The Kondo temperature (6 K) calculated from the parameters used to fit the experimental data is in good agreement with the experimental Kondo line width.

Kondo resonance, the signature around the Fermi level is not so well reproduced.

4. Conclusions

In summary, we have introduced an ionic Hamiltonian for a magnetic atom and shown that it can be used to describe appropriately the inelastic processes associated with the interaction of the magnetic atom and the electrons tunneling between a STM tip and a metal. We have used a Green-function equation of motion method, up to second order in the metal–atom interaction, to analyze those processes; it should be stressed that going beyond that order is necessary to improve the agreement between the theoretical results and the experimental data. Our approach has allowed us to analyze the Kondo resonance (Co case) and the spin excitations of the atom (Fe and Co cases) under an applied bias voltage, with and without a magnetic field. In particular, we have analyzed for the Fe/CuN case its possible $2 \leftrightarrow 3/2$ or $2 \leftrightarrow 5/2$ spin fluctuations, concluding from the step structures and asymmetric spectra that the first is the dominant one. Our analysis for Co/CuN has allowed us to calculate also its Kondo temperature (6 K), a value that is found in good agreement with the experimental evidence.

Acknowledgments

should appear for the Co $3/2 \leftrightarrow 1$ fluctuations, as is found in our calculations (see figure 5); for this case $D = 0.0279$ eV, $E = 0$; $\varepsilon_{S=3/2} - \varepsilon_{S=1} = 1$ eV, $\Gamma_2 = 40$ meV and $\Gamma_1 = 0.7$ meV [2]. Our theoretical calculations show a reasonable agreement with the experimental evidence, although the calculated Kondo resonance at the Fermi energy is somewhat smaller than the experimental one: this is a well-known effect of using a second-order approximation in the equation of motion solution [18]. We can get, however, a good estimation of the Kondo line width T_K, by realizing that for a twofold degeneracy $T_K \approx (\Lambda\Delta)^{1/2} \exp[-\pi |\varepsilon_{3/2} - \varepsilon_1|/2\Delta]$ [15], $\Delta = 5\Gamma_2$ being the d-resonance width. This yields $T_K = 0.5$ meV, in good agreement with the experimental line width of the Kondo resonance. On the other hand, we stress again that the asymmetry observed in the differential conductance at the steps appearing for $\omega = \pm \left(E_1^S - E_m^S\right)$ (figure 5) is due to the different weights associated with the corresponding Green functions: either $\langle n_1^S \rangle$ for G_{11}, or $(-\sum_{k,\alpha,\sigma} \frac{T_{k\alpha\sigma 11} \langle |\varphi_1^S\rangle \langle \varphi_1^{S-1/2}|c_{k\sigma}\rangle}{\tilde{\omega} - \varepsilon_{k\alpha} - E_m^S + E_1^S})$ for G_{m1}. We should also comment that the relevant interaction strengths for the Kondo resonance and the spin fluctuations have the same order of magnitude, as they correspond to the values of $|T_{k,\sigma,j,2}|^2$ and $|T_{k,\sigma,j,m>2}|^2$, respectively. Figure 5 also shows the conductance as a function of the bias voltage for different values of the applied magnetic field B along the hollow direction (B_z). Good agreement with the experimental data is observed for high fields; for low magnetic fields, however, because of the second-order calculation of the
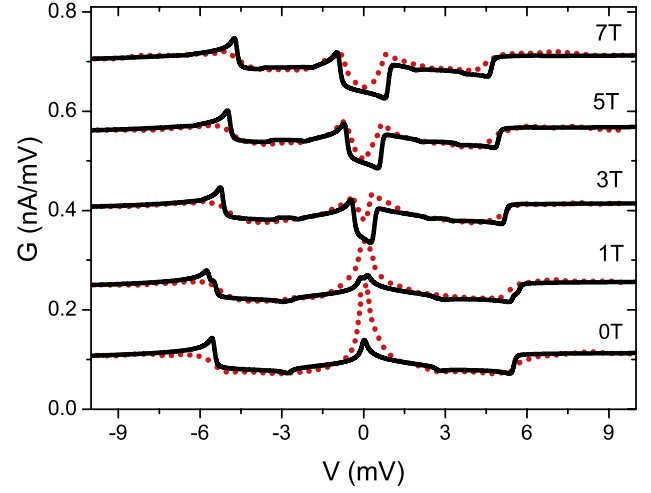
References

[1] Hirjibehedin C F *et al* 2007 *Science* **317** 1199
[2] Otte A F *et al* 2008 *Nature Phys.* **4** 847
[3] Otte A F, Ternes M, Loth S, Lutz C P, Hirjibehedin C F and Heinrich A J 2009 *Phys. Rev. Lett.* **103** 107203
[4] Parks J J *et al* 2010 *Science* **328** 1370
[5] Zyazin A S *et al* 2010 *Nano Lett.* **10** 3307
[6] Persson M 2009 *Phys. Rev. Lett.* **103** 050801
[7] Zitko R and Pruschke Th 2010 *New J. Phys.* **12** 063040
[8] Fernández-Rossier J 2009 *Phys. Rev. Lett.* **102** 256802
[9] Delgado F and Fernandez-Rossier J 2010 *Phys. Rev. B* **82** 134414
[10] Sothmann B and Konig J 2010 *New J. Phys.* **12** 083028
[11] Fransson J, Eriksson O and Balatsky A V 2010 *Phys. Rev. B* **81** 115454

[12] Lorente N and Gauyacq J P 2009 *Phys. Rev. Lett.* **103** 176601
[13] Kondo J 1964 *Prog. Theor. Phys.* **32** 37
[14] Gonzalez G *et al* 2008 *Phys. Rev. B* **78** 054445
Misiorny M *et al* 2011 *Phys. Rev. Lett.* **106** 126602
[15] Hurley A, Baadji N and Sanvito S 2011 *Phys. Rev. B* **84** 115435
[16] Hewson A C 1993 *The Kondo Problem to Heavy Fermions* (Cambridge: Cambridge University Press)
[17] Goldberg E C and Flores F 2008 *Phys. Rev. B* **77** 125121
[18] Goldberg E C, Flores F and Monreal R 2005 *Phys. Rev. B* **71** 035112
Monreal R and Flores F 2005 *Phys. Rev. B* **72** 195105
[19] Keldysh V 1964 *Zh. Eksp. Teor. Fiz.* **47** 1515
Keldysh V 1965 *Sov. Phys. JETP* **20** 1018 (Engl. transl.)
[20] Meyer Y and Wingreen N S 1992 *Phys. Rev. Lett.* **68** 2512